Geomechanics and Engineering, *Vol. 24, No. 4 (2021) 323-335*
DOI: https://doi.org/10.12989/gae.2021.24.4.323

Estimation of the excavation damage zone in TBM tunnel using large deformation FE analysis

Dohyun Kim[1a] and Sangseom Jeong*[2]

[1]*Department of Civil and Environmental Engineering, Massachusetts Institute of Technology, 77 Massachusetts Avenue, Cambridge, 02139, MA, U.S.A.*
[2]*Department of Civil and Environmental Engineering, Yonsei University, 50 Yonsei-ro, Seodaemun-gu, Seoul 03722, Republic of Korea*

(Received March 25, 2020, Revised May 20, 2020, Accepted January 28, 2021)

Abstract. This paper aims to estimate the range of the excavation damaged zone (EDZ) formation caused by the tunnel boring machine (TBM) advancement through dynamic three-dimensional large deformation finite element analysis. Large deformation analysis based on Coupled Eulerian-Lagrangian (CEL) analysis is used to accurately simulate the behavior during TBM excavation. The analysis model is verified based on numerous test results reported in the literature. The range of the formed EDZ will be suggested as a boundary under various conditions – different tunnel diameter, tunnel depth, and rock type. Moreover, evaluation of the integrity of the tunnel structure during excavation has been carried out. Based on the numerical results, the apparent boundary of the EDZ is shown to within the range of 0.7D (D: tunnel diameter) around the excavation surface. Through series of numerical computation, it is clear that for the rock of with higher rock mass rating (RMR) grade (close to 1st grade), the EDZ around the tunnel tends to increase. The size of the EDZ is found to be direct proportional to the tunnel diameter, whereas the depth of the tunnel is inversely proportional to the magnitude of the EDZ. However, the relationship between the formation of the EDZ and the stability of the tunnel was not found to be consistent. In case where the TBM excavation is carried out in hard rock or rock under high confinement (excavation under greater depth), large range of the EDZ may be formed, but less strain occurs along the excavation surface during excavation and is found to be more stable.

Keywords: excavation damaged zone (EDZ); tunnel boring machine (TBM); 3D finite element method (FEM); large deformation analysis; coupled Eulerian-Lagrangian analysis; rock mass rating (RMR); tunnel surface integrity

1. Introduction

In conventional tunneling practice, the excavation process induces not only noise and vibration, but also cracks and fractures on the excavated rock masses, commonly referred to as the excavation damaged zone (EDZ), which threatens the stability of the tunnel as well as the excavation surface. Numerous research facilities, such as Underground Research Laboratory (URL) (Canada), Swedish Nuclear Fuel and Waste Management Corporation (SKB) (Sweden) and Korean Atomic Energy Research Institute (KAERI) (Korea), conducted studies investigating the formation of the EDZ around the excavation surface, and on the changes in physical and material properties. URL has conducted test on the drilling of tunnels and observed formation of fractures and EDZ around the excavation surface (Martin *et al.* 1997, Read *et al.* 1998). SKB performed intensive experiments and field measurements to estimate the formation of the EDZ for conventional drill and blast tunnels and the mechanized tunnels (Bauer *et al.* 1996, Emsley *et al.* 1997). KAERI conducted test and experiments on examining the changes in physical and material properties due to excavation (Kwon *et al.* 2009). The formation of the EDZ is found to be critical to the stability of the tunnel during and after the excavation due to the changes in physical and mechanical property compared to the original rock mass (Arson and Gatmiri 2012, Winberg 1997, Stepansson *et al.* 2008, Siren 2015, Zhang *et al.* 2018, Jeon *et al.* 2020). Moreover, the behavioral characteristics of the EDZ around the excavation surface was found to be dependent not only on the tunnel geometry, but also the dynamic response of the surrounding ground during excavation. The blast vibration in conventional drill and blast method (or the New Austrian Tunneling Method; NATM) and vibration due to the advancement of the TBM will cause severe damage to the ground which will reduce the strength and stability. Therefore, prediction and control of the ground around the excavation surface is critical to the stability of the excavation process (Siren 2015).

Although numerous studies were carried out on the EDZ around the tunnel excavation surface, most of the studies and field measurements were based on conventional drill and blast method. On the contrast, very few studies focused on mechanized tunnels, and attempts to predict the distribution and the range of the EDZ based on numerical analysis are very limited (Read *et al.* 1998, Carbonell *et al.* 2010, Xu and Arson 2014, Kim *et al.* 2015, Lee *et al.* 2016).

Due to the complexity of the TBM tunnel excavation progress and difficulty in accessing the excavation surface,

*Corresponding author, Professor
E-mail: soj9081@yonsei.ac.kr
[a]Ph.D., Post-doctoral researcher
E-mail: geokim@mit.edu

Copyright © 2021 Techno-Press, Ltd.

ISSN: 2005-307X (Print), 2092-6219 (Online)

which is usually concealed by the TBM and the excavated ground, prediction of the EDZ using numerical method prior to the excavation can prevent accidents and delays during excavation. In analyzing the behavior of TBM tunnels during excavation, the latest studies mainly consider the behavior of rock mass during excavation and interaction of the rock mass with the TBM and tunnel lining (Zhao *et al.* 2012). However, the numerical analysis conducted up to date were based on static, discrete sequential analysis, which does not reflect the actual dynamic and continuous behavior of the TBM excavation process. Conventional numerical analysis method (small deformation analysis) has limited capacity in solving the contact surface problems and the excessive deformation of the mesh as the tunnel excavates. To overcome these limitations, and accurately analyze the dynamic behavior of the ground-structure interaction under continuous excavation process, the use of large deformation analysis is necessary (Kim and Jeong 2014, Ko *et al.* 2015).

The advancement of the large deformation analysis techniques is in progress as the capacity of the computers are increasing. Large deformation analysis is widely used for geotechnical matters such as, analysis of driven piles, offshore anchoring process, debris flow and the effect of tunnel excavation on surrounding structures. Various large deformation methods have been developed such as Remeshing and interpolation technique by small strain (RITSS), Adopted mesh (AM) and Coupled Eulerian-Lagrangian (CEL) methods. In this study Coupled Eulerian-Lagrangian (CEL) method was used to analyze the effect of TBM tunnel excavation on surrounding ground.

The main objective of this paper is to 1) predict and suggest the range of the EDZ formation due to TBM excavation by using three-dimensional finite element analysis considering large deformation analysis. The TBM advancing rate and the cutterhead rotation input data is based on actual field practice and various literatures (Chang *et al.* 2006, Cho *et al.* 2010, Hoek and Bieniawski 1965, Hammerer 2013). Verification of the numerical model used in this study will be carried out by comparing the computed results with related field measurements and test results. 2) Effect of various influence factors, such as rock mass, tunnel depth and tunnel diameter will be also examined. Moreover, 3) the stability of the excavation surface will be evaluated to study the direct relationship between the formation of the EDZ and the tunnel stability.

2. Excavation Damage Zone (EDZ)

Due to excavation process, changes in stress distribution around the tunnel occurs and fractures and cracks form in the rock mass. The terminology associated with damaged zones caused by excavation has changed due to enhanced capabilities and understandings of how the damages is induced and how it changes the physical and material properties around the excavations. Generally, the disturbed zone due to excavation can be summarized as shown in Fig. 1 (Perras and Diederichs 2016). Harrison and Hudson (2000) use the terminology of construction damage zone (CDZ), where an inevitable excavation consequences and additional effects occur due to excavation. However, the CDZ can be neglected in most mechanized tunneling process, due to its insignificant range. Zone where it undergoes inevitable damages caused by the result of geometry, structure, and/or induced stress changes (i.e., independent of excavation method) can be defined as the highly damaged zone (HDZ). The HDZ can be typically observed as a zone including interconnection of micro-fractures. Outside the HDZ is normally called the excavation damaged zone (EDZ). The definition of EDZ usually refers to as an area or zone around the excavation surface, where the changes in stress due to excavation exceeds the elastic limit and newly formed fractures or cracks occur. EDZ appears as the tunnel excavates by cracking the rock mass, and this causes reduction of strength and stability of surrounding grounds (Martino *et al.* 2007, Jonsson *et al.* 2009). Siren *et al.* (2015) introduced a concept of excavation influence zone (EIZ), or excavation disturbed zone (EdZ), where it only involves elastic changes degree of stress redistribution.

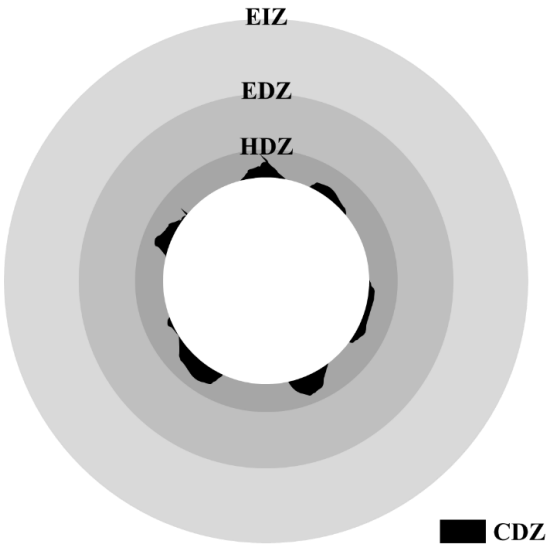

Fig. 1 Excavation damage zones (EIZ, EDZ, HDZ) and construction damage zone

Hoek and Bieniawski (1965) presented the results of the laboratory test on the initiation of a fracture of brittle materials, such as rocks. For materials under uniaxial compression loading condition, the initiation of fracture occurred at about 800% of maximum tensile strength of the material. Additional tests were conducted on various rock types, and the results show that the initiation of fracture occurred at 1500%-2000% of maximum tensile strength. Eberhardt (1998) suggested a stress-strain curve for the rock mass under uniaxial compression loading, as shown in Fig. 2. Diederichs *et al.* (2004) reported an experiment-based field stress ratio (FSR), to determine the crack initiation stress for various rock types, and Martin (1993) suggested an equation which designates the EDZ around the tunnel based on the field stress ratio. Saiang (2004) suggested a model to estimate the EDZ based on field measurements

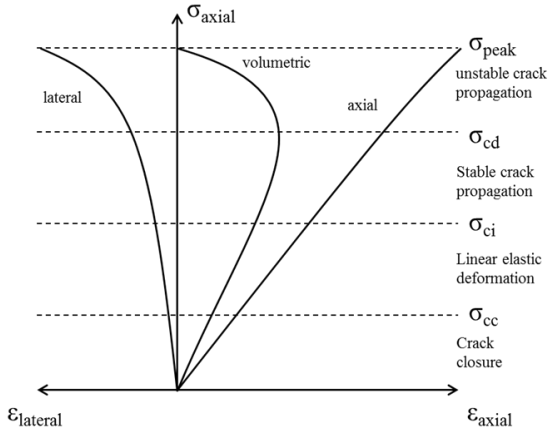

Fig. 2 Stress-strain curve for rock mass under uniaxial compression loading (Eberhardt 1998)

Table 1 Field stress ratio of brittle materials (Diederichs *et al.* 2004)

Rock type	Crack initiation stress (σ_{ci}) / UCS
Indiana limestone	0.320
Concrete	0.330
Lilydale granite	0.345
Pink granite	0.360
Grey granite	0.360
Marble	0.380
Norite	0.405
Granodiorite	0.469
Pegmatite	0.475
Westerly granite	0.476
Chloritized norite	0.496
S.A Quarzite	0.500
Medium sandstone	0.500
Berea sandstone	0.564

and conducted a series of study on the main influence factors on EDZ. Swedish nuclear fuel and waste management conducted a project ZEDEX – Zone of excavation disturbance experiments – to specify the characteristics of EDZ and their behavior and effect on rock conditions due to mechanized excavation as well as conventional tunneling. Siren (2015) compared the difference in the distribution shape and magnitude of EDZ between NATM and TBM tunnels, along with the changes in mechanical properties through field measurements. Some studies attempted to simulate the formation of the EDZ around the mechanized tunnel surface using particle finite element method (PFEM) (Carbonell *et al.* 2010). The formation of the EDZ in TBM tunnel is different from that of NATM tunnel. While EDZ in NATM excavation is caused by instant blast impact on the rock in a wide range, the EDZ during TBM excavation is similar to long-term fatigue failure in a relatively smaller range (Zhang *et al.* 2011, Hardine 2014). Nevertheless, it can be pointed out that most studies have focused on experiments and field measurements after the excavation of the tunnel in defining the EDZ. By contrast, the estimation and prediction of the EDZ using dynamic three-dimensional finite element (FE) method and discussing the relationship between the formation of the EDZ and the stability of the tunnel through numerical evaluation have not been thoroughly presented.

The development of the EDZ around the tunnel excavation surface is critical to the stability during tunnel construction process and the tunnel structure after the completion. Diederichs *et al.* (2004) conducted experiments to define the crack initiation of various rock types (Table 1). The field stress ratio indicates the magnitude of changes in stress in which the new cracks in the rock mass forms, expressed as a portion of the rock mass uniaxial compression stress (UCS). For example, according to the table, if the deviatoric stress in concrete exceeds 33% of the concrete's UCS, newly formed cracks will appear. Martin *et al.* (1993, 2001) suggested a simple equation (Eq. (1)) that under axial loading condition the crack initiation stress is approximately 30-40% of the rocks' uniaxial compression strength based on the field stress ratio results (Fig. 3).

$$\sigma_1' - \sigma_3' = \sigma_{ci} = 30 - 40\% \text{ of } UCS \quad (1)$$

where, σ_{ci} is the crack initiation stress. Based on the Eq. (1), this study has defined the EDZ as an area where the deviatoric stress ($\sigma_1' - \sigma_3'$) caused by the excavation and the dynamic load due to vibration exceeds 30% of the ground's uniaxial compressive strength. This is the lower boundary of the definition of the crack initiation stress based on the field stress ratio, and yield larger EDZ around the excavation surface, thus allowing a safer tunnel design and maintenance.

The schematic of the formation of the EDZ in the numerical analysis conducted in this study is shown in Fig. 4. As the tunnel excavation is in progress, the initial stress (σ_1 or σ_3) around the excavation surface changes ($\sigma_1 + \Delta\sigma$). As the excavation continues, the deviatoric stress ($\Delta\sigma$) increases. In this study assumption is made that, when the deviatoric stress exceeds 30% of the original rocks' uniaxial compression strength, new cracks are formed, thus EDZ appears around the tunnel excavation surface. By using large deformation analysis, the range and the distribution shape of the EDZ under various conditions are investigated.

3. Numerical analysis

In this study, finite element numerical analysis considering large deformation was carried out by using the Coupled Eulerian-Lagrangian (CEL) method to simulate and analyze the effect of TBM tunnel excavation on rock mass.

3.1 Coupled Eulerian-Lagrangian (CEL) method

Small scale FE analysis or the traditional numerical approaches based on a Lagrangian framework, is incapable of simulating the TBM excavation process, where the strain and the displacement of the rock mass is beyond the range of several meters and cause serve mesh distortions and contact problems. Thus, three-dimensional FE analysis considering large deformation is necessary to evaluate the effect of TBM excavation on rock mass and estimate the

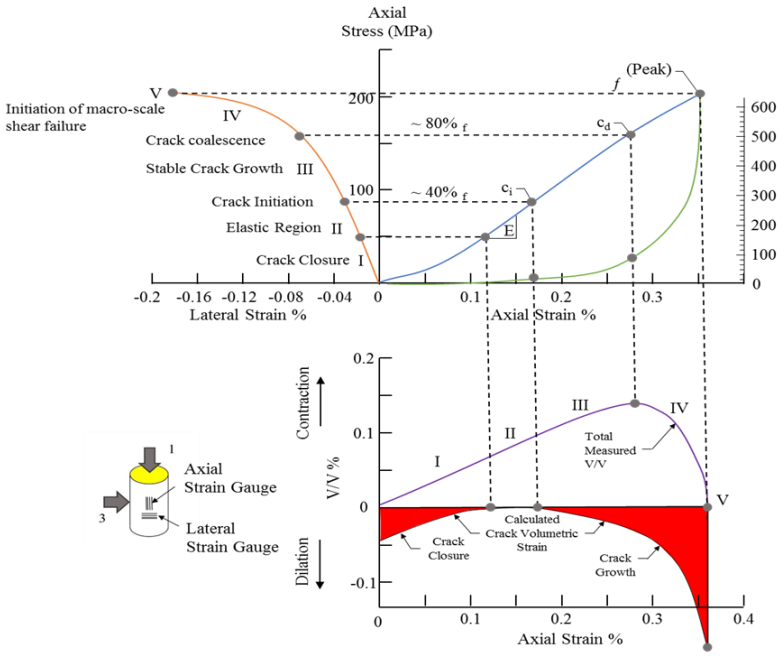

Fig. 3 Stages in the progressive failure of intact rock specimens subjected to compression (Martin *et al.* 2001)

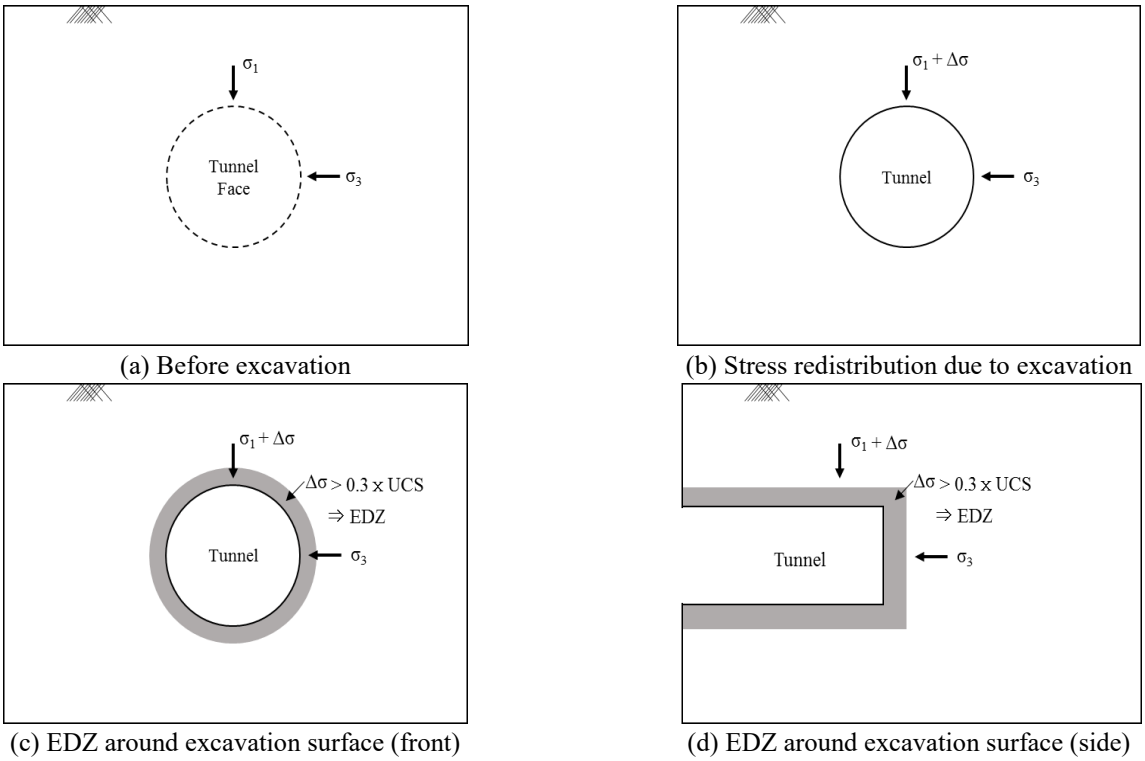

(a) Before excavation

(b) Stress redistribution due to excavation

(c) EDZ around excavation surface (front)

(d) EDZ around excavation surface (side)

Fig. 4 Schematic of the EDZ due to tunnel excavation

distribution and range of the EDZ caused by tunnel excavation. To solve these problems, the Coupled Eulerian-Lagrangian (CEL) method could be applied in simulating and modelling the TBM excavation process. The materials for Lagrangian coordinate which is applied in solid mechanics could not undergo significant deformation, while the materials for Eulerian coordinate which is applied in fluid mechanics could experience large displacements (i.e., soils in tunnel excavation) as Eulerian materials that 'flow' through elements of the stationary mesh (Ko 2015).

The Eulerian equation is based on spatial time derivatives, where the standard Lagrangian equation is based on material time derivatives (Skrzat 2012). To solve the equation, the Lagrangian mass, momentum and energy conservation equations are transferred into the Eulerian conservation equations (Benson and Okazawa 2004). The Eulerian governing equation have the general form as shown in Eq. (2).

$$\frac{\partial \psi}{\partial t} + \nabla \cdot \phi = S \tag{2}$$

where, Φ is the flux function and the S is the source term.

Eq. (2) can be solved sequentially by splitting the Lagrangian and Eulerian terms in to two equations (Benson 1997)

$$\frac{\partial \psi}{\partial t} = S \tag{3}$$

$$\frac{\partial \psi}{\partial t} + \nabla \cdot \phi = 0 \tag{4}$$

where, Eq. (3) contains the source term representing the Lagrangian step, and Eq. (4) contains the convective term representing the Eulerian step. To solve Eq. (3) the deformed mesh from Lagrangian step is moved to the Eulerian fixed mesh, and volume of material transported between adjacent elements is calculated. The Lagrangian solution variables (e.g., mass, stress, energy) are adjusted to account for the flow of the material between adjacent elements. For the Lagrangian step the principle of virtual work is applied (Bathe 1996).

$$\int_V \rho a \cdot \delta u \; dv + \int_V \sigma : \delta \varepsilon \; dV = \int_S t \cdot \delta u \; dS + \int_V \rho b \cdot \delta u \; dV \tag{5}$$

where: $\delta \boldsymbol{u}$ – the virtual displacement, $\delta \boldsymbol{\varepsilon}$ – the virtual strain resulting from virtual displacements, $\boldsymbol{a}$ is the spatial acceleration, and $\boldsymbol{t}$ is the surface traction. In the Lagarangian step, the updated Lagrangian formulation is suitable because the reference configuration (time t) is the current configuration in the Eulerian approach. Unfortunately, in general the configuration of the body at time $t + \Delta t$ considered in Eq. (5) is unknown (unknown is the volume of integration and density which depends on the body deformations). Moreover, the Cauchy stress at time $t + \Delta t$ cannot be obtained by adding to the Cauchy stress at time t the stress increment because the components of the Cauchy stress tensor change when material is subjected to a rigid body rotation. In practice, other strain and stress measures must be used in the principle of virtual displacements; the Green – Lagrange strain tensor and the second Piola-Kirchoff stress tensor (Belytschko *et al.* 2000). The Eulerian material is tracked and calculated as it flows through the mesh by computing its Eulerian volume fraction (EVF). Each Eulerian element is assigned a certain percentage, which means the portion of that element filled with a material. If a Eulerian element is completely filled with a material, the EVF is 1, whereas if there is no material in the element, the EVF is 0. The CEL method that can apply the advantages of both the Lagrangian and the Eulerian method is implemented in commercial software ABAQUS (2013). No re-meshing between steps are required and numerical instability caused by severe mesh distortion is prevented (Tho *et al.* 2012). Fig. 5 shows the deformation of a continuum in a Lagrangian and Eulerian analysis.

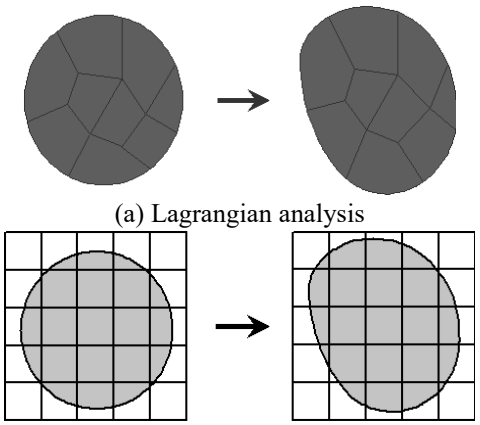

(a) Lagrangian analysis

(b) Eulerian analysis

Fig. 5 Deformation of a continuum in a Lagrangian and a Eulerian analysis

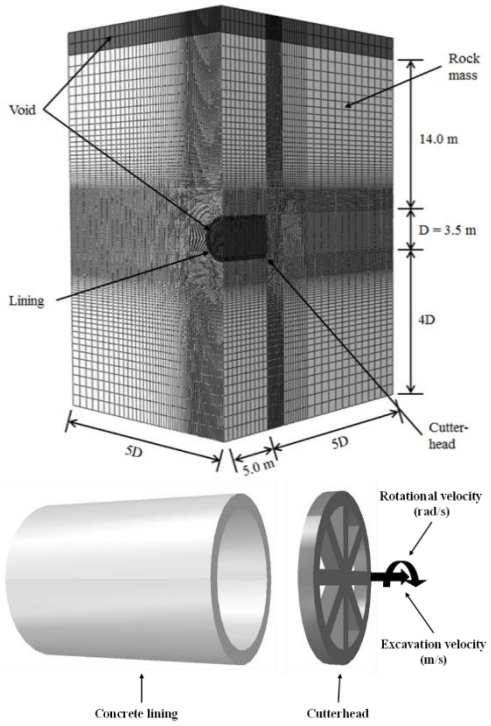

Fig. 6 Schematic of finite-element modeling of ground and TBM

3.2 Coupled Eulerian-Lagrangian (CEL) modeling

As shown in Fig. 6, the modeling of the 3.5 m tunnel was executed below the ground level. The rock was modeled as a Eulerian element, and the mechanical properties were based on the Mohr-Coulomb model. The elements consisting the TBM cutterhead and the lining of the tunnel were modeled as a Lagrangian element, and the properties are shown on Table 2. The initial tunnel length with lining was set to 5 m, and estimation of the EDZ was carried out as the cutterhead rotates and excavates the ground. The lining and the cutterhead was modeled as an 8-node Lagrangian brick element (C3D8R), and the ground was modeled as an 8-node Eulerian brick element (EC3D8R).

Table 2 Material property of lining and cutterhead

	Model (Element)	E (MPa)	v	γ (kN/m^3)
Lining	Linear elastic (Lagrangian)	23,000	0.15	24.0
Cutterhead		200,000	0.30	82.5

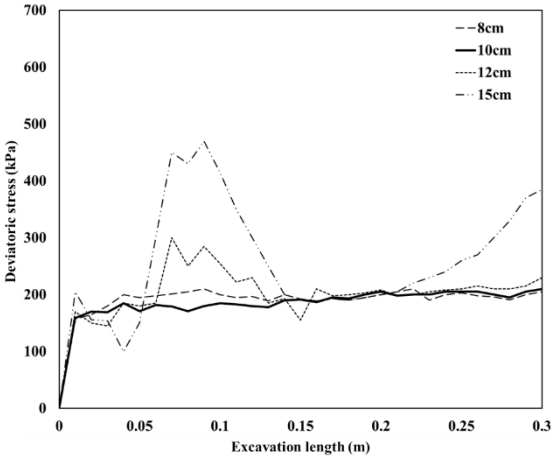

Fig. 7 Results of the convergence study for mesh size

3.3 Mesh and boundary conditions

The mesh and the boundary condition were modeled based on the case studies conducted prior to the actual analysis. The size of the mesh for the finite element analysis was selected to optimize the analysis results and the computation time. Case study showed the results as showed in Fig. 7. Using smaller mesh size yielded accurate results but requires longer computation time. On the other hand, larger mesh size can reduce computation time but shows rough results. Based on the convergence study it was concluded that mesh size of 0.1 m was the maximum value, in which the range of the EDZ was kept constant. For this reason, the single mesh size of 0.1 m was chosen for optimal analysis results and reasonable computation time as shown in Table 3. In addition, based on literature reviews on CEL numerical analysis and series of case studies, the boundary conditions for the analysis were set to 4D in all direction from the tunnel excavation surface to prevent boundary disturbance effect (Kim and Jeong 2014, Ko *et al.* 2015). Prior to the simulation of the TBM excavation, initial geostatic condition was met to reflect the actual soil and rock condition.

3.4 Contact and TBM advancement condition

In finite element analysis, the plasticity of soil is considered through constitutive model, and the most common constitutive model for rock is Mohr-Coulomb model and the Hoek-Brown model.

In this study, the Mohr-Coulomb model was used to analyze the behavior of rocks.

The interface between the Eulerian and Lagrangian elements for CEL analysis are commonly modeled as a general contact. The interfaces between the elements (cutterhead and the rock mass) are modeled as a general

Table 3 Convergence study for optimum mesh size

Minimum mesh size (cm)	D / minimum mesh size	Number of elements	Compute time (hours)
8	43.8	1,591,520	90.35
10	35.0	1,151,796	36.56
12	29.2	680,056	31.05
15	23.3	480,480	19.07

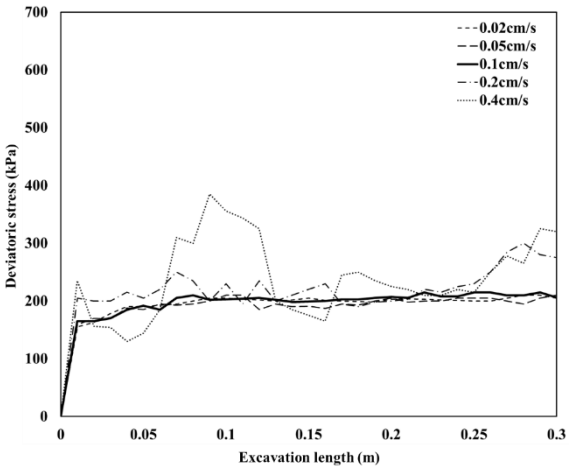

Fig. 8 Results of the convergence study for advance velocity

contact, governed by friction coefficient. The friction coefficient between the elements is set to 0.7, based on literature reviews and previous studies on TBM excavation and the case study in order to estimate the optimal friction coefficient between the cutterhead and the rock mass (Zhao *et al.* 2012, Gehring 1996, Ramoni and Anagnostou 2011). The net velocity of the TBM advancement in the field is approximately 1.8 m/hour ($5x10^{-4}$ m/s). However, if the actual velocity is applied to the analysis, the computation time will be massive. To overcome this limitation, adapting the quasi-static condition and through series of case studies, higher TBM advance velocity could be used in the analysis, and thus significantly reduce the computation time while not affecting the outcome of the results. Fig. 8 shows the effect of the velocity on the outcome in deviatoric stress due to excavation. Results shows that, increasing the TBM advance velocity 10^{-3} m/s does not affect the outcome compared to the actual advance velocity of $5x10^{-4}$ m/s, while the computation time reduces to approximately 25%. For this reason, the TBM velocity in this study was modeled to 10^{-3} m/s to estimate the EDZ around the excavation surface. In addition, the rotation rate of the cutterhead is set to 6rad/s (equivalent to approximately 1RPM) based on field practice recommendations and previous studies (ITA 2000, Lee *et al.* 2016). Based on this, the TBM advancement modeled in CEL approach realistically shows the ground particles being excavated and flowing beyond the modeled cutterhead.

3.5 Model verification

The three-dimensional FE CEL analysis model established in this study was verified prior to the EDZ estimation.

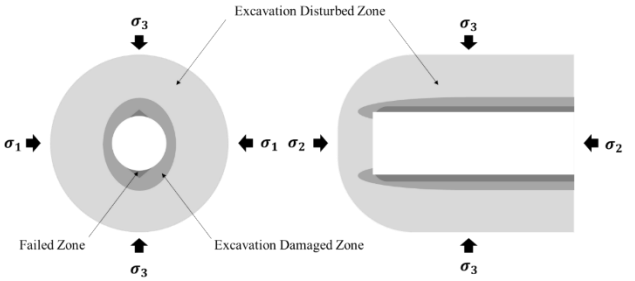

Fig. 9 Schematic of the three-dimensional EDZ around MBE test tunnel (Read 2004)

The model verification was conducted based on literature review and by comparing the analysis result with case studies reported in the literature.

3.5.1 Literature review

Numerous studies on the EDZ around tunnel excavation surface was conducted up to date. The attempts to measure the EDZ around the mechanized tunnel was made under several researches. However, due to the inconvenience in measuring the EDZ during TBM operation, field data based on actual EDZ measurement is severely rare. In addition, difficulty in measuring newly formed micro cracks and fractures due to TBM excavation lead the direct estimation of the EDZ more difficult. For this reason, majority of the studies estimated the EDZ using the changes of seismic wave velocity, thermal and hydraulic conductivity compared to the original rock mass before excavation.

Although not many data are available, general tendency of the shape and the range of the EDZ around mechanized tunnel based on existing studies are as follows:

• Most commonly measured distribution shape of the EDZ around the mechanized tunnel is shown in Fig. 9 (Read 2004). Damage of the surrounding rock mass due to the excavation tends to occur in all direction based on the cross-section view (Emsley *et al.* 1997, Carbonell *et al.* 2010, Read 2004). However, some case results, shown in Fig. 10, indicate that the failed and damaged zone tend to be larger in the upper and lower region of the excavation surface, with a slight larger range showing at the lower location of the tunnel (Siren 2015, Cai and Kaiser 2005, Shen *et al.* 2011). In the front of the excavation surface, the EDZ tend to concentrate in the upper and lower edge, showing a three-dimensional "donut" like shape, if rotated (Martin *et al.* 1997, Emsley *et al.* 1997, Eberhardt 1998, Diederichs *et al.* 2004, Read 2004). This distribution shape of the EDZ is due to the rotation of the cutterhead while excavating, where the stress is concentrated in the edge due to the edge effect (Cai and Kaiser 2005, Blumberg and Tamuzh 1980).

• The magnitude of the EDZ varies according to the rock condition and the excavation condition (TBM velocity and rotation rate). A circular test tunnel was driven in unjointed massive (plutonic) granite using a nonexplosive "non-damaging" excavation procedure developed at the Underground Research Laboratory (URL) operated by the Atomic Energy of Canada Ltd. (AECL). It has been analysed and well documented by numerous researchers

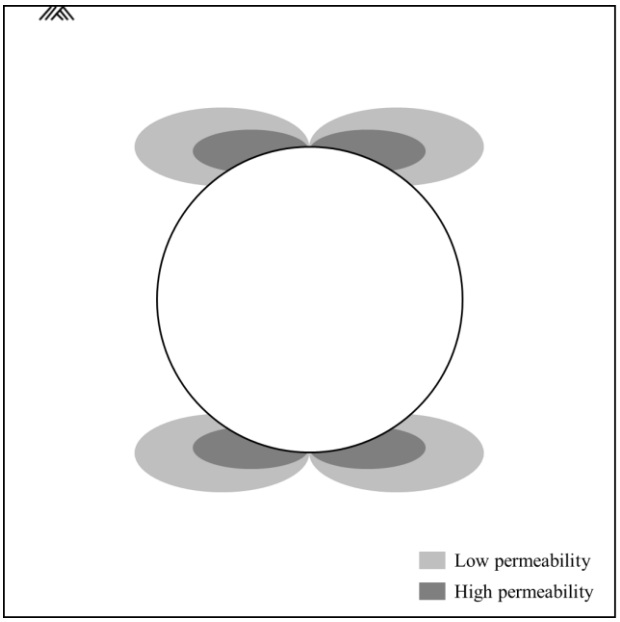

Fig. 10 EDZ around TBM tunnel based on permeability (Emsley *et al.* 1997)

Table 4 Property of verification case study analysis (Read 2004)

Rock type	Density (kN/m^3)	E (GPa)	v	σ_c (MPa)
Granite	26.3	65	0.25	213
Granodiorite	26.6	66	0.25	228

that, the EDZ formed in the range of 0.1-0.5D, where the D is the diameter of the tunnel (Martin *et al.* 1997, Diederichs *et al.* 2004, Martin 1989, Cundall *et al.* 1996, Martino and Chandler 2004). Based on the measured results, Diederichs *et al.* (2004) estimated the EDZ around the mechanized tunnel using the crack initiation and propagation theory. Through estimation, the distribution shape and the range of the EDZ field measurements were justified (Eberhardt 1998).

3.5.2 Comparing with field case study

Fig. 11 is the representative result of the EDZ forming around the TBM excavation surface, where the grey area is the region where the deviatoric stress exceeds 30% of the original rock mass, the threshold of the EDZ. The analysis was conducted under the identical condition (Table 4) of the 3.5m diameter MBE (Mine-by-experience) test tunnel operated by the Atomic Energy of Canada Ltd. (AECL) (Read *et al.* 1998, Read 2004). In the analysis, the average of two rock types' mechanical property was considered.

As seen in Fig. 11(a), the EDZ at the front of the excavation surface is concentrated in the upper and lower zone in front of the excavation surface. Identical results can be seen in the MBE test tunnel experiment. The EDZ yielded by the numerical analysis will also form a "donut" shape (if rotated in three-dimension) with a slightly large EDZ on the bottom of the TBM, which is reported in the literature. However, as seen in Fig. 9(b), the cross-section view (seen from the back of the TBM) the EDZ was more concentrated in the crown and the lower region of the

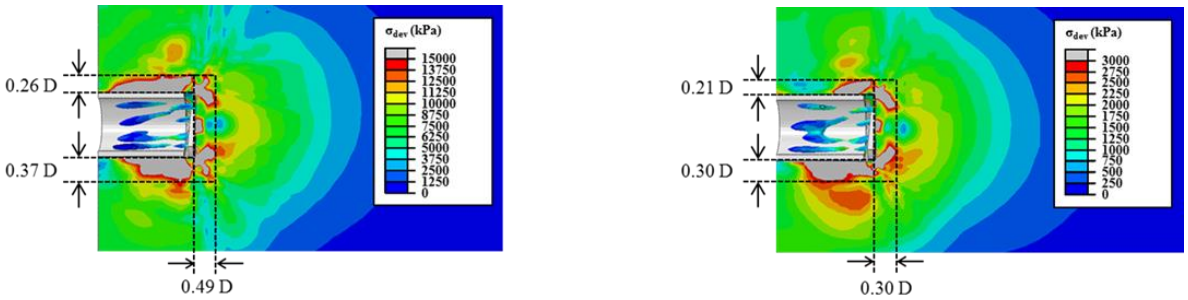

RMR 2nd grade RMR 4th grade

(a) Side view of the CEL analysis

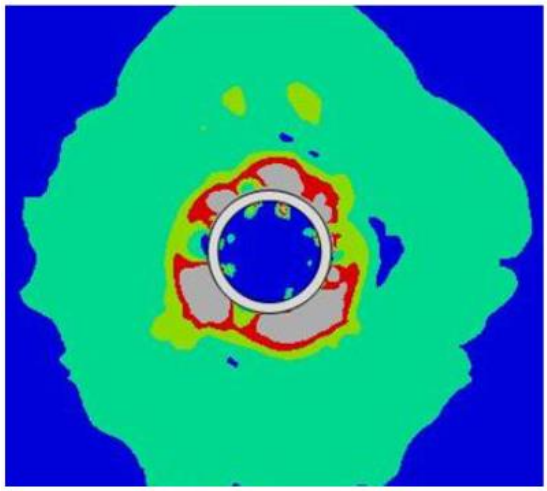

(b) Section view of the CEL analysis

Fig. 11 Representation of the EDZ due to TBM excavation using CEL analysis

tunnel. The similar distribution of the EDZ was reported in the field measurement conducted by numerous studies including Emsley *et al.* (1997) and Read (2004). The range of the formation of the EDZ obtained from the numerical model analysis was also found to be within the results stated in the MBE test.

Based on the literature reviews and series of numerical analysis conducted in this study, the range of the EDZ computed based on the CEL analysis is in good agreement with the field measurements and theoretical estimation. Through comparison, it can be concluded that the numerical model used in this study can be adequately used to simulate the actual behavior of the TBM excavation process and estimate the distribution shape and range of the EDZ around the excavation surface.

4. Estimation of the EDZ range and tunnel stability evaluation

In this study, estimation of the EDZ range around the tunnel based on large deformation analysis was carried out for various tunnel diameters, tunnel depths, and rock conditions. Table 5 summarizes the 54 numerical cases conducted. The typical grading and properties of rock based on the RMR grades and weathered rock are stated in Table 6 (Bieniawski 1993, Jeong *et al.* 2014). The ground was modeled as a homogeneous rock, since it was found that the homogeneous rock condition yielded the largest EDZ based on prior numerical case studies, thus can be applied as conservative (safer) excavation practice. The TBM excavation advancement velocity and the cutterhead rotation rate was modeled to 1.67×10^{-3}m/s, 0.3 rpm, respectively. The range of the EDZ was designated as a region where the deviatoric stress due to the excavation exceeds 30% of the original rock mass uniaxial compression strength (Diederichs *et al.* 2004). Through numerical computation, the range of the EDZ will be shown separately for the upper, lower and in front of the TBM tunnel, normalized by dividing the maximum range of the EDZ (m) by the tunnel diameter(D). Moreover, the stability of the excavation surface will be evaluated by analyzing the tunnel strain level. The tunnel will be defined as 'unstable' if the strain of the excavation surface induced due to the TBM advancement exceeds 1% of tunnel diameter (Sakurai 1983, Chern *et al.* 1998).

4.1 Estimation of the EDZ range

Based on the 54 cases of numerical analysis, the range of the EDZ around the tunnel was estimated and the effect of major influence factors – such as tunnel diameter, depth, and rock type – was studied. The results of the numerical computation on the EDZ range around the tunnel, normalized in tunnel diameter, is shown Table 7 and Fig. 12.

Table 5 Summary of numerical cases

	Diameter (m)	Depth (m)	Rock mass rating (RMR)
1	2.5	17.5 (5D)	1st grade
2	3.5	35.0 (10D)	2nd grade
3	4.5	70.0 (20D)	3rd grade
4	-	-	4th grade
5	-	-	5th grade
6	-	-	Weathered rock

Table 6 Summary of rock properties based on rock mass ratings (Bieniawski 1993, Jeong *et al.* 2004)

Group	RMR	E (MPa)	UCS (MPa)	ν	γ (kN/m3)	φ (°)	c (kPa)
I	80~100	20,000	75	0.20	27	45	4,000
II	61~80	10,000	50	0.22	26	40	2,000
III	41~60	6,000	30	0.24	25	35	1,000
IV	21~40	2,000	10	0.26	23	32	400
V	< 20	800	4	0.28	22	30	100
W.R	-	200	2	0.30	21	32	50

*W.R: Weathered rock

Table 7 Numerical results of the EDZ formation (Upper/Lower/Front)

Rock type (rock mass rating)	Depth		
	5 D (m/D)	10 D (m/D)	20D (m/D)
1st grade	0.70 / 0.72 / 0.58	0.35 / 0.51 / 0.25	0.28 / 0.42 / 0.17
2nd grade	0.40 / 0.45 / 0.42	0.21 / 0.28 / 0.17	0.17 / 0.22 / 0.11
3rd grade	0.25 / 0.39 / 0.30	0.12 / 0.22 / 0.13	0.09 / 0.17 / 0.07
4th grade	0.20 / 0.30 / 0.22	0.07 / 0.15 / 0.11	0.04 / 0.09 / 0.05
5th grade	0.18 / 0.29 / 0.15	0.05 / 0.13 / 0.07	0.03 / 0.07 / 0.03
Weathered rock	0.15 / 0.25 / 0.09	0.03 / 0.10 / 0.03	0.02 / 0.05 / 0.02

*The results stated in the table is an average value of tunnels with different diameters. For example, the range of the EDZ at the upper location of the tunnel on RMR 1st grade rock excavated 5 D below the surface (0.70) is an average value of 0.71D1 (D1=2.5 m), 0.71D2 (D2=3.5 m), and 0.72D3 (D3=4.5 m)

Tunnel diameter was found to be in near exact direct proportional relationship with the range of the EDZ. For this reason, if the results were normalized with the tunnel diameter the variation among the cases between different diameters was within ±5%, which can be assumed as insignificant.

The depth of the tunnel was found to have a notable effect on the size of the EDZ around the tunnel. As the TBM excavation is executed deeper below the surface, from 5D depth to 20D depth, the size of the EDZ was smaller in all directions than the tunnel near the surface. This result is due to the fact that, rock in greater depth has higher uniaxial compression strength and higher confinement stress. Moreover, the decrease rate in size of the EDZ was shown more significant in relatively weak weathered rock.

The propagation of vibration in rock mass, which is closely related to the formation of EDZ during TBM excavation, is greatly affected by the discontinuity of rock mass. However, assuming that the rock contains no discontinuity (yielding maximum range of EDZ), the vibration generally travels faster, thus longer distance in hard intact rock with higher elastic modulus (Shiwa and Kishi 2005, Eitzenberger 2012). The numerical computation carried out in this study is in good agreement with preceding studies and researches. It was found that the range of the EDZ around the TBM tunnel during excavation was larger in relatively harder rocks. However, even though the vibration due to TBM advancement caused more cracks in harder rocks, the stability of the tunnel can be threatened in the case where the excavation is conducted in weak weathered rock. Further analysis and investigation will be stated by tunnel stability evaluation.

Overall, it was evident that the formation of the EDZ during TBM excavation was also significant, which can cause negative effect on the tunnel structure.

4.2 Evaluation of tunnel stability

In additional to estimating the range of the EDZ, stability of the tunnel was evaluated and investigated, which may be more critical and practical in actual engineering practice.

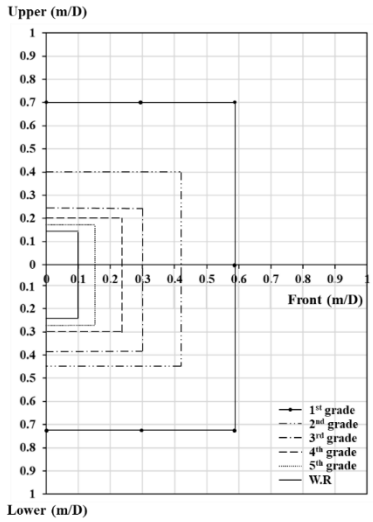

(a) Formation of the EDZ range (at 5D depth)

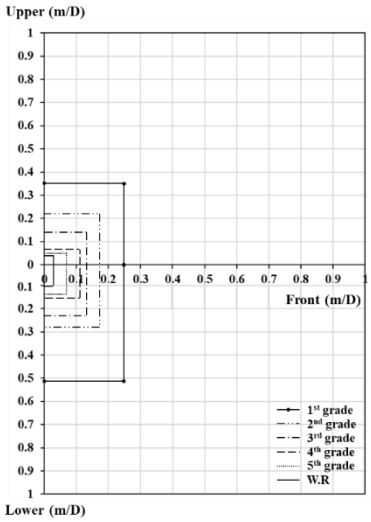

(b) Formation of the EDZ range (at 10D depth)

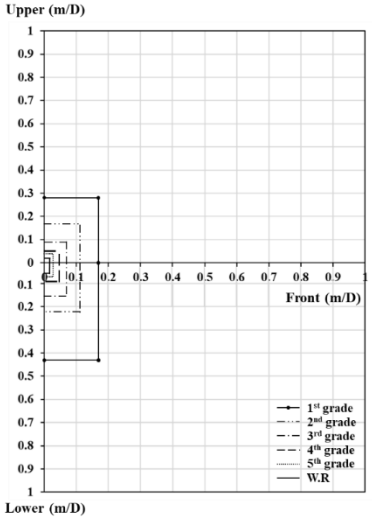

(c) Formation of the EDZ range (at 20D depth)

Fig. 12 Results of the EDZ estimation due to TBM excavation

Table 8 Tunnel stability analysis (D=2.5 m/3.5 m/4.5 m)

Rock type (rock mass rating)	Depth		
	5 D (Max. strain)	10 D (Max. strain)	20 D (Max. strain)
1st grade	< 1%	< 1%	< 1%
2nd grade	< 1%	< 1%	< 1%
3rd grade	< 1%	< 1%	< 1% / 1.1% / 1.0%
4th grade	2.0% / 2.2% / 2.1%	2.5% / 2.5% / 2.7%	2.6% / 2.7% / 2.7%
5th grade	3.6% / 3.6% / 3.5%	4.3% / 4.4% / 4.9%	5.0% / 5.0% / 5.2%
Weathered rock	10.8% / 9.6% / 9.7%	12.9% / 13.3% / 13.5%	15.9% / 16.5% / 16.7%

Based on observations and measurements, Sakurai (1983) suggested that tunnels with strain level over 1% may be associated with the onset of tunnel instability and with difficulties in providing adequate degree of support, and this suggestion was confirmed by field observations (Chern *et al.* 1998). Even though some tunnels which suffered strains exceeding 5% did not show stability problems, it was clear that construction problems increased significantly with increasing strain level over 1%. For this reason, the 1% limit in indicating the instability of tunnel was applied in the analysis.

Table 8 shows the results of the strain level of the tunnels through large deformation analysis. It was evidently shown that, even though larger size of the EDZ was estimated to form around the tunnel for harder rock conditions, the stability of the tunnel was not compromised

for RMR 1st and 2nd grade rocks, where strain level was limited below 1%. For RMR 3rd grade condition, strain level exceeding 1% only appeared where the depth of the tunnel was 20D. However, for rocks of 1st through 3rd grade was found to be overall stable, despite the broad formation of the EDZ. As for the rocks below the 4th grade to weathered rock, the numerical prediction indicated that the strain caused by the TBM excavation was over the 1% limit. Especially, in case of TBM excavation in weathered rocks, it was found to be extremely unstable, showing over 10% of strain level for most cases due to TBM excavation. In addition, the strain of the tunnel was found to be higher as the tunnel depth increases. This may be caused by the high in-situ earth pressure acting on the tunnel. Based on the results, it shown to be necessary to install linings and reinforcements (rock bolts, shotcrete, etc.) for deep tunnel excavation on relatively weaker rocks (Eftekhari and Aalianvari 2019). Finally, if normalized by the tunnel diameter, the results were found to be constant, which means the tunnel diameter has a direct proportional relation with the strain level similar to the formation of the EDZ.

5. Conclusions

In this study, the range of the EDZ around TBM tunnel excavation surface was investigated by using three-dimensional large deformation analysis method. To simulate the dynamic, complex, and continuous process of the TBM excavation and the damage it causes on a rock mass, large deformation numerical analysis based on CEL method was used. In addition, the advance velocity and the rotation rate of the cutterhead was based on actual TBM operating practice standard. Moreover, the evaluation of the tunnel strain was conducted to study the relation between the EDZ and the tunnel stability. Based on previous studies and series of numerical analysis, the following conclusions can be drawn:

• By applying the threshold of the EDZ to a region where the deviatoric stress due to the excavation exceeds 30% of the original rock mass uniaxial compression strength, the range of the EDZ was estimated for upper, lower, front location of the tunnel, normalized with the tunnel diameter (m/D). It was clear that the lower parts of the TBM yielded the largest range of the EDZ.

• Verification of the applied numerical model was based on experimental tests and preceding studies, due to no apparent field measurements of the EDZ during actual TBM advancement. The analysis model used in this study was found to be capable of accurately estimating not only the distribution shape the EDZ, but also the size and range of the EDZ as well.

• Numerical studies on the effect of main influence factors – rock type, tunnel diameter and tunnel depth – were investigated. Based on the numerical computation results, the range of the EDZ around the TBM tunnel differs according to the rock types. As the RMR grade gets lower (i.e, as the rock mass is weaker), the normalized range (m/D) of the EDZ tends to decrease. Also, under extremely high earth pressure environment (deeper below the surface), the TBM excavation causes smaller EDZ. The tunnel diameter was found to be in direct proportional relationship with the size of the EDZ formed due to the TBM excavation.

• By analyzing the strain level during TBM excavation, it was concluded that the formation of the EDZ does not always results in degrading of the tunnel stability. Even though the size of the EDZ was shown to form largest in harder rock masses (RMR 1st – 3rd grade rocks) due to stress redistribution or faster and longer propagation of the TBM excavation vibration, the strain level was limited to 1%, and the integrity and the stability of the tunnel was not violated. As for the weaker rock masses, the EDZ was shown in smaller range but the strain level exceeded the 1% limit – in weathered rock, up to 16% – which can be an indicator of an unstable tunnel structure.

• Although the formation for the EDZ due to TBM excavation may be kept in limited sizes compared to the conventional drill-and-blast method, it can still cause significant degree of the EDZ around the excavation surface. However, the size may not be the indication of the instability of the tunnel structure. In TBM tunnels within deep depth below the surface on weak rock masses (i.e, below RMR 4th grade, including weathered rock), special attention and reinforcement should be necessary in TBM practice.

Acknowledgments

This work was supported by the Basic Science Research Program through the National Research Fund of Korea (NRF) (No. 2018R1A6A1A08025348) and the Ministry of Land, Infrastructure and Transport (Grant No. 19SCIP-B119955-014-000000) of the Republic of Korea, and we express our gratitude.

References

ABAQUS CAE (2013), *ABAQUS User's Manual*, Dessault Systemes Simulia Corporation, Rhode Island, U.S.A.

Arson, C. and Gatmiri, B. (2012), "Thermo-hydro-mechanical modeling of damage in unsaturated porous media: Theoretical framework and numerical study of the EDZ", *Int. J. Numer. Anal. Meth. Geomech.*, **36**(3), 272-306. https://doi.org/10.1002/nag.1005.

Bathe, K.J. (1996), *Finite Element Procedures*, Klaus-Jurgen Bathe, Upper Saddle River, New Jersey, U.S.A.

Bauer, C., Homand-Etienne, F., Ben Slimane, K., Hinzen, K.G. and Reamer, S.K. (1996), "Damage zone characterization in the near field in the Swedish ZEDEX tunnel using in situ and laboratory measurements", *Proceedings of the Eurock '96,* Turin, Italy, September.

Belytschko, T., Liu, K. and Moran, B. (2000), *Non-linear Finite Element Analysis for Continua and Structures*, John Wiley & Sons, New York, U.S.A.

Benson, D.J. and Okazawa, S. (2004), "Contact in a multi-material Eulerian finite element formulation", *Comput. Meth. Appl. Mech. Eng.*, **193**, 4277-4298. https://doi.org/10.1016/j.cma.2003.12.061.

Bieniawski, Z.T. (1993), *Classification of Rock Masses for Engineering: The RMR System and Fracture Trends*, in *Comprehensive Rock Engineering*, Pergamon Press, 553-574.

Blumberg, N.N. and Tamuzh, V.P. (1980), "Edge effects and stress concentrations in multilaminate composite plates", *Mech. Compos. Mater.*, **16**(3), 298-307. https://doi.org/10.1007/BF00608331.

Cai, M. and Kaiser, P.K. (2005), "Assessment of excavation damaged zone using a micromechanics model", *Tunn. Undergr. Sp. Tech.*, **20**(4), 301-310. https://doi.org/10.1016/j.tust.2004.12.002.

Carbonell, J., Onate, E. and Suarez, B. (2010), "Modeling of ground excavation with the particle finite-element method", *J. Eng. Mech.*, **136**(4), 455-463. https://doi.org/10.1061/(ASCE)EM.1943-7889.0000086.

Chang, S.H., Choi, S.W., Bae, G.J. and Jeon, S. (2006), "Performance prediction of TBM disc cutting on granitic rock by the linear cutting test", *Tunn. Undergr. Sp. Tech.*, **21**(3), 271-281. https://doi.org/10.1016/j.tust.2005.12.131.

Chern, J.C., Yu, C.W. and Shiao, F.Y. (1998), "Tunnelling in squeezing ground and support estimation", *Proceedings of the Regular Symposium of Sedimentary Rock Engineering*, Taipei, Tawian.

Cho, W.J., Jeon, S., Yu, S.H. and Chang, S.H. (2010), "Optimum spacing of TBM disc cutters: A numerical simulation using the three-dimensional dynamic fracturing method", *Tunn. Undergr. Sp. Tech.*, **25**(3), 230-244. https://doi.org/10.1016/j.tust.2009.11.007.

Cundall, P.A., Potyondi, D.O. and Lee, C.A. (1996), "Micromechanics-based models for fracture and breakout around the mine-by tunnel", *Proceedings of the Canadian Nuclear Society International Conference on Deep Geological Disposal of Nuclear Waste*, Winnipeg, Canada, September.

Diederichs, M.S., Kaiser, P.K. and Eberhardt, E. (2004), "Damage initiation and propagation in hard rock during tunneling and the influence of near-face stress rotation", *Int. J. Rock Mech. Min. Sci.*, **41**, 785-812. https://doi.org/10.1016/j.ijrmms.2004.02.003.

Eberhardt, E.D. (1998), "Brittle rock fracture, progressive damage in uniaxial compression", Ph.D. Thesis, University of Saskatchewan, Saskatchewan, Canada.

Eftekhari, A. and Aalianvari, A. (2019), "An overview of several techniques employed to overcome squeezing in mechanized tunnels; A case study", *Geomech. Eng.*, **18**(2), 215-224. https://doi.org/10.12989/gae.2019.18.2.215.

Eitzenberger, A. (2012), "Wave propagation in rock and influence of discontinuities", Ph.D. Thesis, Lulea University of Technology, Lulea, Sweden.

Emsley, S., Olsson, O., Stenberg, L., Alheid, H.J. and Falls, S. (1997), *ZEDEX – A Study of Damage and Disturbance from Tunnel Excavation by Blasting and Tunnel Boring*, Swedish Nuclear Fuel and Waste Management CO, Sweden.

Gehring, K.H. (1996), *Design criteria for TBM's with Respect to Real Rock Pressure. Tunnel Boring Machines—Trends in Design & Construction of Mechanized Tunneling, International Lecture Series TBM Tunnelling trends*, Hagenberg. AA Balkema, Rotterdam, The Netherlands, 43-53.

Hammerer, N. (2013), "Influence of steering actions by the machine operator on the interpretation of TBM performance data", Research Report, Pennsylvania State University, Pennsylvania, U.S.A.

Hardine, E. (2014), "Review of underground construction methods and opening stability for repositories in clay/shale media", Research Report, Sandia National Laboratories, New Mexico, U.S.A.

Harrison, J.P. and Hudson, J.A. (2000), *Engineering Rock Mechanics: Part 2: Illustrative Worked Examples*, Elsevier.

Hoek, E. and Bieniawski, Z.T. (1965), "Brittle fracture propagation in rock under compression", *Int. J. Fract. Mech.*, **1**(3), 137-155. https://doi.org/10.1007/BF00186851.

Jeon, Y.J., Jeon, S.C., Jeon, S.J. and Lee, C.J. (2020), "Study on the behaviour of pre-existing single piles to adjacent shield tunnel by considering the changes in the tunnel face pressures and the location of the pile tips", *Geomech. Eng.*, **21**(2), 187-200. https://doi.org/10.12989/gae.2020.21.2.187.

Jeong, S.S., Han, Y.C., Kim, Y.M. and Kim, D.H. (2014), "Evaluation of the NATM tunnel load on concrete lining using the ground lining interaction model", *KSCE J. Civ. Eng.*, **18**(2), 672-682. https://doi.org/10.1007/s12205-014-0597-9.

Jonsson, M., Backstrom, A., Feng, Q., Berglund, J., Johansson, M. and Olsson, M. (2009), "Aspo hard rock laboratory: studies of factors that affect and controls the excavation damage/disturbed zone", SKB Report R-09-17, Swedish Nuclear Fuel and Waste Management CO, Sweden.

Kim, D.H., Jeong, S.S. and Kim, K.Y. (2015), "FEM based estimation of EDZ under TBM induced vibration", *Proceedings of the ITA World Tunnel Congress 2015*, Dubrovnik, Croatia, May.

Kim, Y.H. and Jeong, S.S. (2014), "Analysis of dynamically penetrating anchor based on coupled Eulerian-Lagrangian (CEL) methods", *J. Kor. Soc. Civ. Eng.*, **34**(3), 895-906. https://doi.org/10.12652/Ksce.2014.34.3.0895.

Ko, J.Y. (2015), "Evaluation of bearing capacity for open-ended piles with soil plugging", Ph.D. Dissertation, Yonsei University, Seoul, Korea.

Kwon, S.K., Lee, C.S., Cho, S.J., Jeon S.W. and Cho, W.J. (2009), "An investigation of the excavation damaged zone at the KAERI underground research tunnel", *Tunn. Undergr. Sp. Tech.*, **24**(1), 1-13. https://doi.org/10.1016/j.tust.2008.01.004.

Lee, S.Y., Kim, D.H. and Jeong, S.S. (2016), "A study on the excavation damage zone (EDZ) under TBM advancement based on large deformation technique (Coupled Eulerian-Lagrangian)", *J. Kor. Geotech. Soc.*, **32**(10), 5-13. https://doi.org/10.7843/kgs.2016.32.12.5.

Martin, C.D. (1989), "Failure observations in situ stress domains at the Underground Research Laboratory", *Proceedings of the Conference on Rock Mechanics and Rock Physics at Great Depth*, Pau, France, August-September.

Martin, C.D. (1993), "The strength of massive Lac du Bonnet granite around underground openings", Ph.D. Dissertation, University of Manitoba, Manitoba, Canada.

Martin, C.D., Christiansson, R., and Soderhall, J. (2001), "Rock stability considerations for siting and constructing a KBS-3 repository: Based on experiences from Aspo HRL, AECL's URL, Tunneling and mining", Swedish Nuclear Fuel and Waste Management CO, Sweden.

Martin, C.D., Read, R.S. and Martino, J.B. (1997), "Observation of brittle failure around a circular test tunnel", *Int. J. Rock Mech. Min. Sci.*, **34**(7), 1065-1073. https://doi.org/10.1016/S1365-1609(97)90200-8.

Martino, J.B. and Chandler, N.A. (2004), "Excavation-induced damage studies at the Underground Research Laboratory", *Int. J. Rock Mech. Min. Sci.*, **41**(8), 1413-1426. https://doi.org/10.1016/j.ijrmms.2004.09.010.

Martino, J.B., Dixon, D.A., Kozak, E.T., Gascoyne, M., Vignal, B., Sugita, Y., Fujita, T. and Masumoto, K. (2007), "The tunnel sealing experiment: An international study of full-scale seals", *Phys. Chem. Earth*, Parts A/B/C, **32**(1-7), 93-107. https://doi.org/10.1016/j.pce.2006.04.023.

Perras, M.A. and Diederichs, M.S. (2016), "Predicting excavation damage zone depths in brittle rocks", *J. Rock Mech. Geotech. Eng.*, **8**(1), 60-74. https://doi.org/10.1016/j.jrmge.2015.11.004.

Ramoni, M. and Anagnostou, G. (2011), "The interaction between shield, ground and tunnel support in TBM tunnelling through squeezing ground", *Rock Mech. Rock Eng.*, **44**(1), 37-61. https://doi.org/10.1007/s00603-010-0103-8.

Read, R.S. (2004), "20 years of excavation response studies at AECL's Underground Research Laboratory", *Int. J. Rock Mech. Min. Sci.*, **41**(8), 1251-1275. https://doi.org/10.1016/j.ijrmms.2004.09.012.

Read, R.S., Chandler, N.A. and Dzik, E.J. (1998), "In situ strength criteria for tunnel design in highly-stressed rock masses", *Int. J. Rock Mech. Min. Sci.*, **35**(3), 261-278. https://doi.org/10.1016/S0148-9062(97)00302-1.

Saiang, D. (2004), "Damaged rock zone around excavation boundaries and its interaction with shotcrete", Licentiate Thesis, Lulea University of Technology, Sweden.

Sakurai, S. (1983), "Displacement measurements associated with the design of underground openings", *Proceedings of the International Symposium of Field Measurements in Geomechanics*, Zurich, Switzerland, September.

Shen, B., Stepansson, O., Rinne, M., Amemiya, K., Yamashi, R., Toguri, S., and Asano, H. (2011), "FRACOD modeling of rock fracture and permeability change in excavation damaged zones", *Int. J. Geomech.*, **11**(4), 302-313. https://doi.org/10.1061/(ASCE)GM.1943-5622.0000034.

Shiwa, M. and Kishi, T. (2005), *Encyclopedia of Materials: Science and Technology*.

Siren, T. (2015), "Excavation damage zones, fracture mechanics simulation and in situ strength of migmatitic gneiss and pegmatitic granite at the nuclear waste disposal site in Olkiluoto", Ph.D. Dissertation, Aalto University, Espoo, Finland.

Skrzat, A. (2012), "Application of coupled Eulerian-Lagrangian approach in metal forming simulations", *Zeszyty Naukowe Politechniki Rzeszowskiej*, **284**, 25-35. https://doi.org/10.7862/rm.2012.9.

Stepansson, O., Shen, B., Rinne, M., Amemiya, K., Yamashi, R., and Toguri S. (2008), "FRACOD modeling of rock fracture and permeability change in excavation damaged zones", *Proceedings of the 12th International Conference of International Association for Computer Methods and Advances in Geomechanics (IACMAG)*, Goa, India, October.

Tho, K.K., Leung, C.F., Chow, Y.K. and Swaddiwedhipong, S. (2012), "Eulerian finite-element technique for analysis of jack-up spudcan penetration", *J. Geotech. Geoenviron. Eng.*, **12**(1), 64-73. https://doi.org/10.1061/(ASCE)GM.1943-5622.0000111.

Winberg, A. (1997), "The role of the disturbed rock zone in radioactive waste repository safety and performance assessment. A topical discussion and international overview", Swedish Nuclear Fuel and Waste Management CO, Sweden.

Xu, H. and Arson, C. (2014), "Anisotropic damage models for geomaterials: Theoretical and numerical challenges", *Int. J. Comput. Meth.*, **11**(2), https://doi.org/10.1142/S0219876213420,073.

Zhang, C., Chu, W., Liu, N., Zhu, Y., and Hou, J. (2011), "Laboratory tests and numerical simulations of brittle marble and squeezing shist at Jinping II hydropower station China", *J. Rock Mech. Geotech. Eng.*, **3**(1), 30-38. https://doi.org/10.3724/SP.J.1235.2011.00030.

Zhang, Y., Ding, X., Huang, S., Yang, Q., Peng, L. and Li, Y. (2018), "Field measurement and numerical simulation of excavation damage zone in a 2000 m-deep cavern", *Geomech. Eng.*, **16**(4), 399-413. https://doi.org/10.12989/gae.2018.16.4.399.

Zhao, K., Janutolo, M. and Barla, G. (2012), "A completely 3D model for the simulation of mechanized tunnel excavation", *Rock Mech. Rock Eng.*, **45**(4), 475-497. https://doi.org/10.1007/s00603-012-0224-3.